Journal of Cellular Biochemistry 79:311–321 (2000)

Tyrosine Phosphorylation and Cellular Redistribution of Ezrin in MDCK Cells Treated With Pervanadate

Yi-Xin Wu,* Tadayoshi Uezato, and Michiya Fujita

Department of Biochemistry, Hamamatsu University School of Medicine, 3600 Handa-cho, Hamamatsu-shi, Japan

Abstract Ezrin is a key protein in membrane-cytoskeleton interaction and is expressed primarily in actin-rich surface projections. Activation in protein tyrosine phosphorylation apparently regulates the structure and function of ezrin. In this study, we found that pervanadate (PV, the complexes of vanadate with hydrogen peroxide) caused an increase in tyrosine phosphorylation of ezrin and affected its cellular redistribution. Treatment of Madin-Darby canine kidney (MDCK) cells with pervanadate resulted in a dramatically increased tyrosine phosphorylation of ezrin within two to five min and the level reached the maximum after 60 min. This was accompanied by an alteration in the subcellular distribution of ezrin. Immunofluorescence and scanning laser confocal microscopy analysis revealed that, after PV stimulation, ezrin was redistributed from cytosol to the apical and lateral membrane domains. This occurred within five min, and more obvious redistribution to the lateral membrane domain was observed after 30 min. Furthermore, immunoblotting of ezrin in cell fractionation experiments showed that, in PV-treated MDCK cells, cytosolic ezrin was translocated to the membrane fraction, while there was no change in the level of ezrin associated with the actin-cytoskeleton. Therefore, cytoplasmic signaling may result in activation of ezrin in tyrosine phosphorylation, which is induced by PV stimulation. These results suggest that ezrin has qualities that might play a role in modulation of cell shape and adhesion. J. Cell. Biochem. 79:311–321, 2000.

Key words: MDCK cell; pervanadate; ezrin; protein tyrosine kinase; protein tyrosine phosphatase

INTRODUCTION

Ezrin and radixin moesin constitute the ezrin-radixin-moesin (ERM) protein family. On the basis of the homology ERM proteins have with erythrocyte band 4.1 protein and cytoskeletal localization, it is thought that the ERM proteins serve as membrane-cytoskeleton linkers [Algrain et al., 1993; Funayama et al., 1991]. Ezrin is the most studied member of the ERM family, and shares approximately 75% primary sequence identity at the amino acid level [Funayama et al., 1991]. The interaction of ezrin between membrane proteins and the cytoskeleton has been identified. The results indicated that it can bind to various integral membrane proteins including CD 44 [Tsukita et al., 1994], CD 34 [Yonemura et al., 1998], ICAM-2 [Helander et al., 1996], and ICAM-3 [Yonemura et al., 1998] via its N-terminal domain, and binds to F-actin via its C-terminal domain. Additionally, recent studies suggested that ezrin is involved in cell-cell and cell-substrate adhesions [Crepaldi et al., 1997; Takeuchi et al., 1994; Wu et al., 1996].

The proteins at the boundary between the cytoskeleton and the plasma membrane control cell shape, delimit specialized membrane domains, and stabilize attachments to other cells and to the substrate. It is of interest to note that these proteins also regulate cell locomotion and cytoplasmic responses to growth factors and other external stimuli [Luna and Hitt, 1992]. The ERM family of proteins, of which ezrin is the most studied member, is thought to function as the membrane-cytoskeletal linker [Mangeat et al., 1999]. Changes in protein phosphorylation in tyrosine, as well as in serine/threonine residues, apparently regulate the structure and function of ERM proteins [Bretscher, 1989; Crepaldi et al., 1997; Hirao et al., 1996]. Epidermal growth fact (EGF) and hepatocyte growth factor (HGF) stimulate tyrosine phos-

*Correspondence to: Yi-Xin Wu, Deptartment of Biochemistry, Hamamatsu University School of Medicine, 3600 Handa-cho, Hamamatsu-shi, Japan. E-mail: yixinwu@hama-med.ac.jp

Received 31 August 1999;Accepted 24 March 2000

phorylation of ezrin [Bretscher, 1989; Jiang et al., 1995]. In a MDCK cell line transfected with a temperature-sensitive mutant of v-src (ts-v-src MDCK), the activation of ts-v-src increases the tyrosine phosphorylation level ERM proteins [Takeda et al., 1995]. In addition, ezrin-tyrosine phosphorylation might be mediated by the actions of protein tyrosine phosphatase (PTPase). In Jurkat T cells, only after pretreatment with PTPase inhibitors (PV, the complexes of vanadate with hydrogen peroxide +PAO, phenylarsine oxide) did T-cell antigen receptor (TCR) ligation stimulate tyrosine phosphorylation of ezrin [Egerton et al., 1992]. In the EGF treatment system, incubation with PAO enhanced the degree of ezrin-tyrosine phosphorylation, and increased the amount of ezrin oligomer formed [Berryman et al., 1995]. These findings suggest that tyrosine phosphorylation of ezrin might occur under various physiological conditions, although the knowledge regarding the precise mechanism is still limited.

PV, a PTPase inhibitor, was shown to cause increases in tyrosine phosphorylation and various cell signaling responses [Ayalon and Geiger, 1997; Gilbert-McClain et al., 1998; Huyer et al., 1997; Ruff et al., 1997; Wilden and Broadway, 1995]. We were interested in whether ezrin is tyrosine phosphorylated in the presence of PTPase inhibitors, and in cellular responses to such signals. Here, we examined the effects of the PTPase inhibitor PV on MDCK cells and found that ezrin is involved in responses to tyrosine phosphorylation signals.

MATERIALS AND METHODS

Cell Culture and Materials

MDCK cells were obtained from RIKEN Cell Bank and maintained in Dulbecco's modified Eagle's medium (DMEM) supplemented with 10% (v/v) fetal bovine serum (GIBCO-BRL) at 37°C under 5% CO_2 in humidified air. Sodium orthovanadate was from Sigma.

Antibodies

Ezrin was purified from human placenta, as described previously by Bretscher [1989]. The polyclonal (pAb) antiezrin antibody was raised in rabbits using the purified human ezrin. Mouse monclonal (mAb) antiezrin antibody clone:18 was purchased from Transduction Laboratories. Monoclonal antiphosphotyrosine antibody PY 20 was from ICN Biomedicals. Rodamine phalloidin was from Molecular Probes, Inc. Texas Red-conjugated goat antimouse IgG was from Jackson Immunoresearch Labs. Fluorescin isothiocyanate (FITC)-conjugated goat antirabbit IgG was from Zymed.

PV Treatment

Confluent MDCK cell monolayers were washed three times with serum-free DMEM, then 0.1 mM H_2O_2 and 0.1 mM sodium orthovanadate in serum-free medium were added to the cells and incubated for different periods of time. Cells were lysed in RIPA buffer [20 mM Tris-HCl (pH 7.4), 150 mM NaCl, 0.1% (w/v) SDS, 1% (v/v) Triton X-100, 1% (w/v) deoxycholic acid, 10 mM NaF, 1 mM Na_3VO_4, 5 mM EDTA, 1 mM phenylmethylsulfonyl fluoride (PMSF), 10 μg/ml leupeptin, and 10 μg/ml aprotinin]. Protein concentration was determined using a BCA kit (Pierce) and equal amounts of protein were subjected to SDS-PAGE and analyzed by Western immunoblotting.

Immunoprecipitation

Cultured cells were treated with PV at 37°C. At the end of the incubation period, cells were rinsed three times with ice cold PBS^- (phosphate-buffered saline without Mg^{2+} and Ca^{2+}) and lysed on ice for 30 min in RIPA buffer. Cell lysates were clarified by centrifugation at 10,000 × *g* for 30 min. After determining the protein concentration, equal amounts of protein from clarified cell lysates were incubated with 5 μl rabbit polyclonal antiezrin antibody protein for two h at 4°C. Protein A-Sepharose (Pharmacia) was then added for one hour. Immune complexes were washed three times with RIPA buffer (lysis buffer), eluted by boiling in Laemmli sample buffer [Laemmli, 1970], and analyzed by SDS-PAGE and Western immunoblotting.

Electrophoresis and Western Blotting

SDS-PAGE was performed according to Laemmli [1970]. After electrophoresis, the gels were transferred to nitrocellulose filters (Hybond ECL, Amersham) for immunoblotting. The membranes were blocked with 5% (w/v) dry skim milk in TBST buffer [20 mM Tris-HCl (pH 7.5), 150 mM NaCl, and 0.05% Tween-20] for one h. After washing in TBST buffer, the filters were probed with primary antibodies

(antiezrin or PY 20) in 1% (w/v) skim milk/TBST buffer for one h at room temperature. The primary antibody reactions were detected with peroxidase-conjugated goat antirabbit or antimouse IgG in 1% skim milk/TBST buffer, and developed using an enhanced chemiluminescence Western blotting kit (ECL, Amersham) according to the manufacturer's specifications. For reprobing, the filters were stripped by a 10 min incubation at 60°C in stripping buffer [62.5 mM Tris-HCl (pH 6.8), 2% SDS, and 100 μM 2-mercaptoethanol], blocked in 5% dry skim milk in TBST buffer, and probed as described above.

Immunocytochemistry

MDCK cells grown on glass coverslips were fixed in 3percnt; paraformaldehyde in PBS^+ (phosphate-buffered saline containing 0.5 mM $CaCl_2$ and 0.5 mM $MgCl_2$) for 20 min at room temperature. The fixed cells were washed and then permeabilized by incubation with 0.5% (v/v) Triton X-100 in PBS^+ for 10 min. After washing, the cells were incubated for 30 min in PBS^+containing 1% (w/v) bovine serum albumin (BSA). Incubation with primary antibodies was in PBS^+ containing 1% BSA for one h at room temperature. After washing, the cells were then incubated for 30 to 60 min at room temperature with Texas Red or FITC-conjugated secondary antibody and mounted. Coverslips were examined with a Zeiss Axioscope microscope. For scanning laser confocal analysis, cells labeled with fluorescence were viewed with a laser scanning confocal system (BioRad MRC 600) through a 60 × oil immersion objective. The data were analyzed using Comos software. Images were converted to tagged information file format (TIFF), and processed using Photoshop software (Adobe) on a Power Macintosh 9500 (Apple).

Extraction of Cells with Detergent/Salt Solutions

Confluent monolayers of cells were subjected to a modified protocol described previously [Bush et al., 1994; Stuart et al., 1996], which yields two fractions: soluble (S) and salt-sensitive cytoskeleton (C). After incubation in PV, monolayers were briefly rinsed twice with a buffer containing 10 mM Tris-HCl (pH 7.5), 150 mM NaCl, and 1 mM PMSF. Cells were extracted for 15 min at 4°C on a rotating platform after covering the cells with CSK-1 buffer [containing 0.5% Triton X-100, 10 mM Tris-HCl (pH 7.5), 100 mM NaCl, 300 mM sucrose, 10 mM NaF, 1 mM Na_3VO_4, and a proteinase inhibitor mixture]. The extract (S-fraction) was aspirated, and the monolayers were further extracted under the same conditions with CSK-2 buffer, which differs from CSK-1 buffer only in that it contains 1 M NaCl in place of 100 mM NaCl. The second extract (C-fraction) was separated. Equivalent aliquots of soluble and insoluble fractions were analyzed by Western immunoblotting.

For immunoprecipitation of ezrin, each of the C-fractions was diluted with CSK-1 buffer without NaCl to a final concentration of 100 mM NaCI. After that, both the soluble and cytoskeleton fractions were clarified by centrifugation at 10,000 × *g* for 30 min. Equivalent aliquots of soluble and insoluble fractions were immunoprecipitated with antiezrin pAb, and the immunoprecipitates were separated by SDS-PAGE and immunoblotting.

Preparation of Cell Extracts

MDCK cells were then rapidly washed with ice-cold PBS^-, scraped, and collected by centrifugation at 1,000 × *g* for 10 min. Preparation of cell extracts was performed as described previously [Warne et al., 1995]. The collected cells were lysed briefly by sonication in ice cold homogenization buffer [20 mM Tris-HCl (pH 7.5), 2 mM dithiothreitol, 10 mM NaF, 1 mM Na_3VO_4, 2 mM EDTA, 0.5 mM EGTA, 0.33 M sucrose, and a protease inhibitor mixture]. The suspension was separated into a cytosol fraction by ultracentrifugation (100,000 × *g* for 60 min). The pellet was suspended in homogenization buffer containing 5 mg/ml Triton X-100, and the extracted membrane fraction (supernatant) was separated by ultracentrifugation (100,000 × *g* for 60 min). After determining the protein concentration, equal amounts of protein for both fractions were analyzed by Western immunoblotting.

For immunoprecipitation of ezrin protein, Triton X-100 was added to both the cytosol and membrane fractions to a final concentration of 1% (v/v). Each fraction was incubated for 30 min on ice, and then clarified by centrifugation at 10,000 × *g* for 30 min. Equal amounts of protein from each clarified fraction were immunoprecipitated with antiezrin pAb or PY 20,

and the immunoprecipitates were separated and immunoblotting.

RESULTS

Characterization of Antibodies to Human Ezrin

Ezrin was purified from human placenta essentially as described by Bretscher [1989]. After the last purification step, fractions from a Mono S column, a single peak of 81-kDa proteins were obtained (Fig. 1A). This 81-kDa protein was then subjected to amino-terminal sequencing. The resulting sequence, MPKPINVRVTTMDA, indicated that the purified 81-kDa protein was human ezrin, as described previously [Bretscher, 1989]. Polyclonal antibodies were then elicited in rabbit immunized with this purified 81-kDa ezrin protein. Since the previous studies indicated that ezrin and radixin are very similar in their deduced amino acid sequences [Funayama et al., 1991], we further examined our antiezrin pAb are specific for ezrin and not for radixin. Results of the immunoprecipitation analysis using this antibody in MDCK cells is shown in Fig. 1B, Line 2. The results revealed that a protein with a single band apparent molecular mass at 81-kDa was specifically immunoprecipitated. Furthermore, the immunoprecipitates from MDCK cells was also examined by immunoblotting with another antiezrin mAb that was previously characterized as specifically recognizing ezrin. The data showed that antiezrin mAb reacted against this immunoprecipitate (Fig. 1B). Moreover, antibodies were characterized by immunoblotting on a variety of cell lines (Fig. 1C). Western blot analysis of homogenates from cultured MDCK, LLC-PK$_1$, porcine kidney cells, Caco-2, and Madin-Darby bovine kidney (MDBK) cells showed that the ezrin pAb specifically reacted with a single band at 81-kDa (Fig. 1C). Altogether, these results indicate that this polyclonal antibody specifically recognizes ezrin.

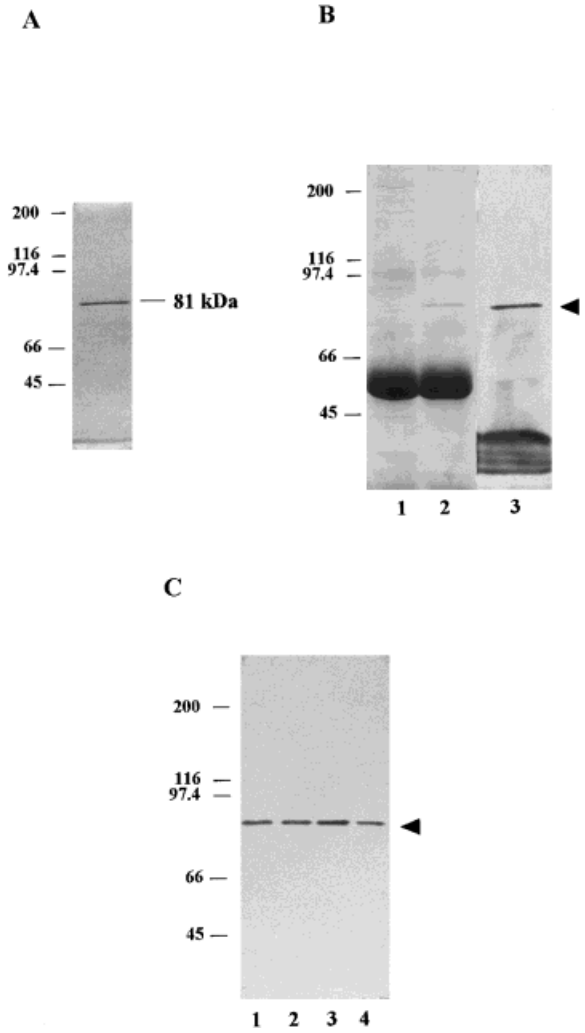

Fig. 1. Characterization of ezrin-specific antibodies. **A:** one μg sample of purified 81-kDa protein from Mono S column was resolved by 10% SDS-PAGE and stained with Coomassie blue. **B:** Cultured MDCK cells were lysed and then immunoprecipitated with antiserum raised against human placental ezrin. The resulting immunoprecipitates, with control rabbit IgG (**Lane 1**) and antiezrin pAb (**Lane 2**), were resolved on a 10% SDS-PAGE and stained with Coomassie blue. To detect ezrin, the immunoprecipitates were blotted with antiezrin mAb (**Lane 3**). **C:** Total cell extracts from the following cell lines were separated by 10% SDS-PAGE, transferred to nitrocellulose, and probed with antibody raised against human placental ezrin. **Lane 1**, MDCK cells; **lane 2**, LLC-PK$_1$ cells; **lane 3**, Caco-2 cells; **lane 4**, MDBK cells. Arrow indicates the migration of ezrin.

Tyrosine Phosphorylation in PV-Treated MDCK Cells

Pervanadate treatment increased levels of tyrosine phosphorylation in MDCK cells as determined by immunoblotting assay (Fig. 2A). A significant level of phosphorylation was apparent after two to five min, and the levels increased with longer incubations (Fig. 2A). Western blot analysis indicated that stimulation with PV dramatically augmented phosphorylation of a large number of protein bands, ranging in molecular mass from 20 to 200 kDa. However, the changes in phosphorylation levels of different protein bands varied significantly. These included a gradual increase in the phosphorylation levels of some bands (e.g. 180, 120, 110, 80, 50, and 30 kDa) peaking at 15 to 60 min (Fig. 2A). The

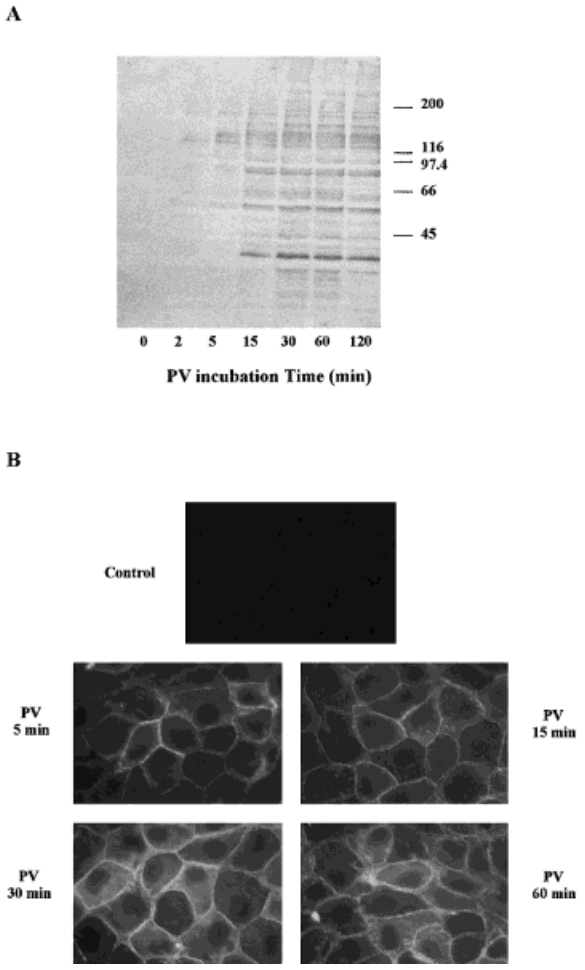

Fig. 2. Effect of PV stimulation on the presence of P-Tyr in MDCK cells. **A:** Cultured MDCK cells were incubated with 100 mM PV. Total protein extracts at indicated times were separated by 10% SDS-PAGE and transferred to a nitrocellulose filter. Immunoblots were probed with anti-P-Tyr antibody (PY 20). The mobility of protein size markers is indicated in kDa **B:** MDCK cells grown on glass coverslips were incubated with 100 mM PV for the indicated times. Cells were fixed and processed for immunofluorescence using PY 20 antibody and then observed through an immunofluorescence microscope. Photographs were taken at a magnification of 1,000 ×.

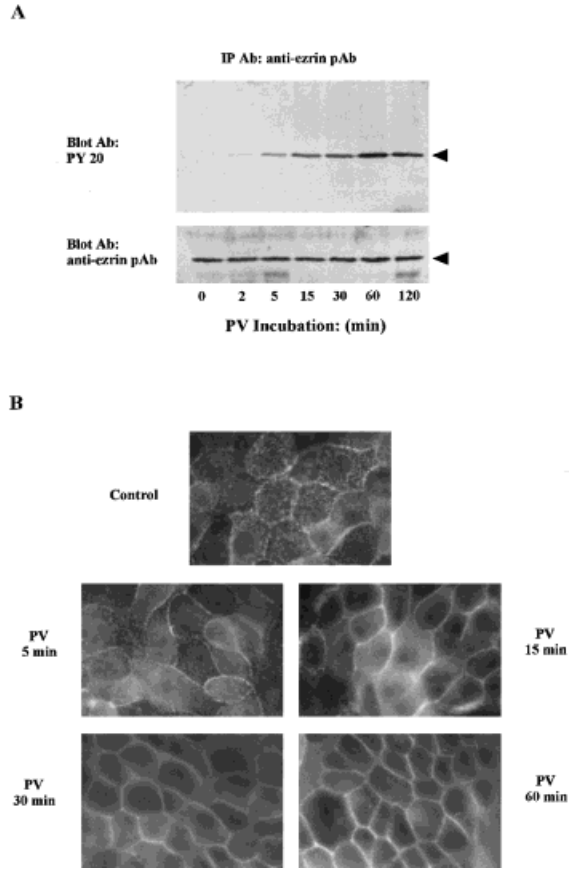

Fig. 3. Effect of PV stimulation on ezrin tyrosine phosphorylation and distribution in MDCK cells. **A:** MDCK cells were incubated with 100 mM PV. The cells were lysed and immunoprecipitated using antiezrin pAb. The immunoprecipitates were blotted with PY 20 (upper panel) and reprobed with antiezrin antibody on the same membrane filter (lower panel). Arrow indicates the migration of ezrin. **B**: MDCK cells grown on glass coverslips were incubated with 100 mM PV for the indicated times. Cells were fixed and processed for immunofluorescence using antiezrin antibody and then observed through an immunofluorescence microscope. Photographs were taken at a magnification of 1,000 ×.

immunocytochemical analysis using antiphosphorylation antibody is shown in Fig. 2B. In control MDCK cells, there was not detectable with tyrosine phosphorylation (Fig. 2B, control). However, a five min treatment with PV resulted in an intensely-labeled line at the periphery of nearly all cells. Longer exposure (15 min) with PV revealed that the phosphotyrosine (P-Tyr)-containing components were associated specifically with areas of intercellular contact (Fig. 2B). After a 30-min incubation, the MDCK cells were relatively intensely stained with the antibody. Diffuse cytoplasmic staining was also apparent after 15 min of incubation.

PV Stimulated Tyrosine Phosphorylation of Ezrin

To address the issue of the identity of ezrin phosphorylated in response to PV treatment, a polyclonal antibody was raised that specifically recognized ezrin as described above. Ezrin was immunoprecipitated using the antiezrin pAb and the tyrosine phosphorylated ezrin was detected by immunoblotting. PV treatment clearly stimulated tyrosine phosphorylation of ezrin (Fig. 3A). There was a dramatic increase

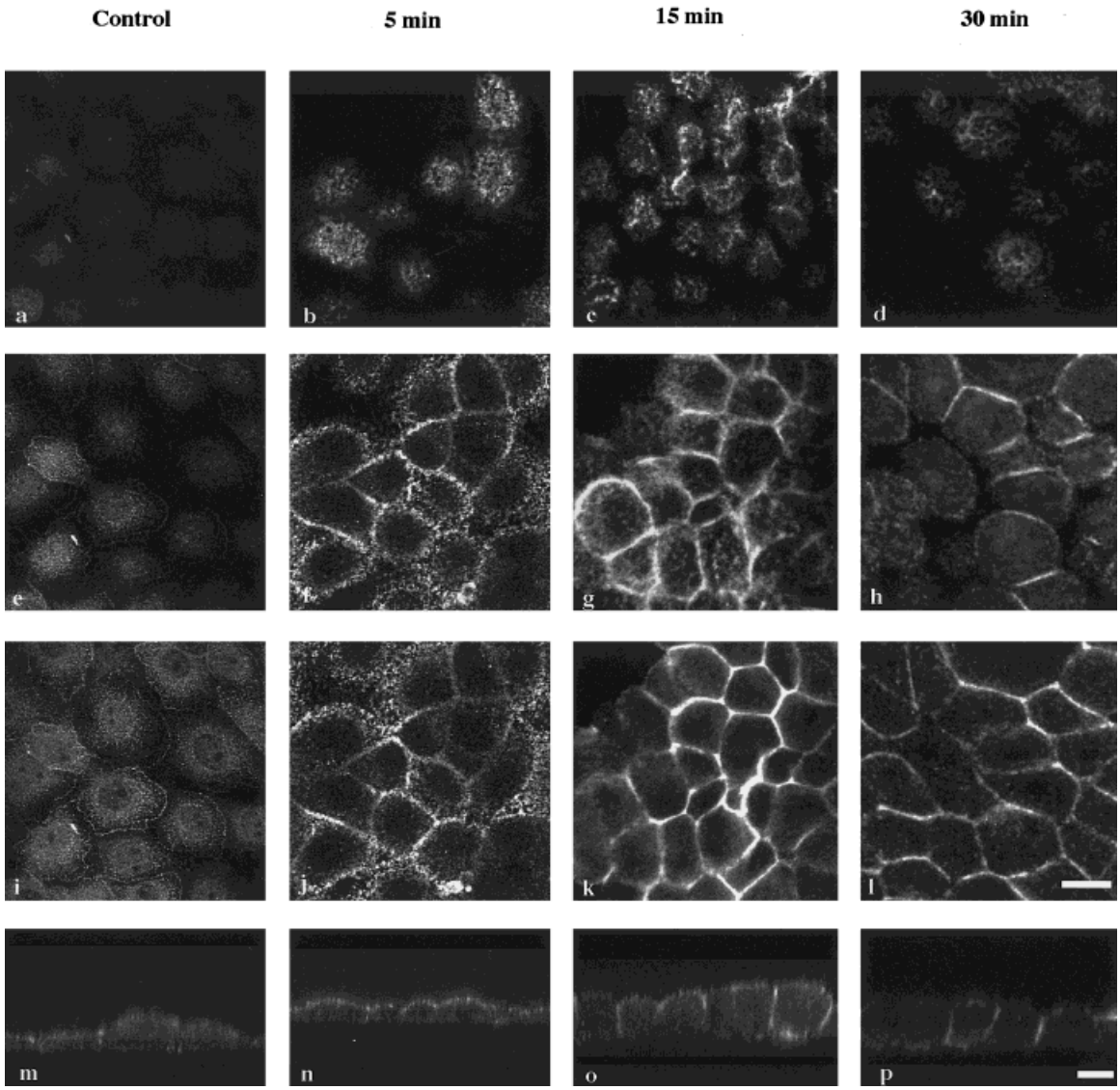

Fig. 4. Confocal microscope images of MDCK cells showing the distribution of ezrin in control and PV-treated MDCK cells. MDCK cells grown to confluence on coverslips were incubated with 100 mM PV for the indicated times and stained with antiezrin pAb. Serial x-y horizontal focal sections (parallel through MDCK cells) were performed from apical (**A-D**) to near the center level (**E-L**) of the cells. The lower panel shows x-z sections (**M-P**) taken in 0.15 mM steps through the cells at 90° to the x-y sections (selected area same as in x-y sections). Pictures were obtained with a BioRad MAC 600 confocal microscope, converted to TIFF images, and processed identically by Adobe Photoshop program with identical settings. Scale bar, 10 mM.

in the level of ezrin-phosphotyrosine in response to treatment with PV. Tyrosine phosphorylated ezrin levels rapidly increased within two to five min and reached maximal values at 60 min of incubation (Fig. 3A). These immunoprecipitates were also examined by immunoblotting with the antiezrin pAb on the same membrane filter. The results showed that the ezrin was tyrosine phosphorylated in response to PV without a change in the recovered amount of ezrin protein.

Cellular Redistribution of Ezrin Occurred After PV Treatment

The effect of PV treatment on the localization of ezrin in MDCK cells was examined with both immunofluorescence microscopy (Fig. 3B) and

scanning laser confocal analysis (Fig. 4). In non-PV-treated control cells, ezrin was localized in the cytosol, the microvilli, and along the lateral surface at cell-cell boundaries (Figs. 3B and 4A, E, I, and M). When cultured MDCK cells were treated with 100 mM PV, the distribution of ezrin was altered. Treatment with PV for five min caused an increase in ezrin staining at cell surface structures. As shown in Fig. 3B, after PV incubation, ezrin staining was increased at apical and cell-cell boundaries. Serial x-y horizontal optical sections show an increase in ezrin staining at apical and cell-cell contacts (Fig. 4B, F, and J). The same conclusions were derived from x-z vertical sections (Fig. 4N). After 15 min of incubation, a further increase in ezrin staining was observed at cell surface structures. As shown in Fig. 3B, ezrin staining was more intense at cell borders. The scanning laser confocal analysis showed that ezrin was clearly recruited into the cell peripheries and that increased staining of ezrin was observed at cell-cell contacts (Fig. 4G, K, and O). After incubation for 30 min with PV, a decline in ezrin staining at the apical structure was noted, but strong staining of ezrin at cell-cell contacts was observed for almost all cells (Figs. 3B and 4H, I, and P). In contrast to the dramatic increase in the level of ezrin labeling at the cell surface structures, cytoplasmic staining of ezrin appeared to decline after incubation for five min with PV (Figs. 3B and 4). These data suggest that PV treatment might cause a redistribution of cytosolic ezrin to the cell surface structures.

In addition, it seems that PV treatment induced morphological cell changes. In confocal x-z vertical section views, the thickness of the monolayer of MDCK cells was increased (Fig. 4M-P). This would imply that PV treatment might be involved in the regulation of total plasma membrane and might induce a cell to round up.

Another tyrosine-specific phosphatase inhibitor, PAO, which causes tyrosine phosphorylation of proteins associated with intercellular junctions in MDCK cells, was also used. However, PAO failed to stimulate the tyrosine phosphorylation of ezrin (data not shown).

Association of Ezrin With the Cytoskeleton Does Not Change After PV Stimulation

The previous studies indicated that PV stimulation induced reorganization of the actin association system [Volberg et al., 1992]. Considering that ezrin is an actin-cytoskeleton-associated protein, it was necessary to determine whether redistribution of ezrin, which was dependent on tyrosine phosphorylation induced by PV treatment, still occurred after disruption of its association with the actin-cytoskeleton. We examined the Triton X-100 solubility of ezrin after PV stimulation. MDCK cells were lysed and divided into two fractions: soluble (S) and salt-sensitive cytoskeleton (C). Ezrin was immunoprecipitated using antiezrin pAb and tyrosine phosphorylation was examined by immunoblotting. As shown in Fig. 5A, PV clearly brought about a dramatic increase in the phosphotyrosine levels of ezrin in both the soluble and cytoskeleton

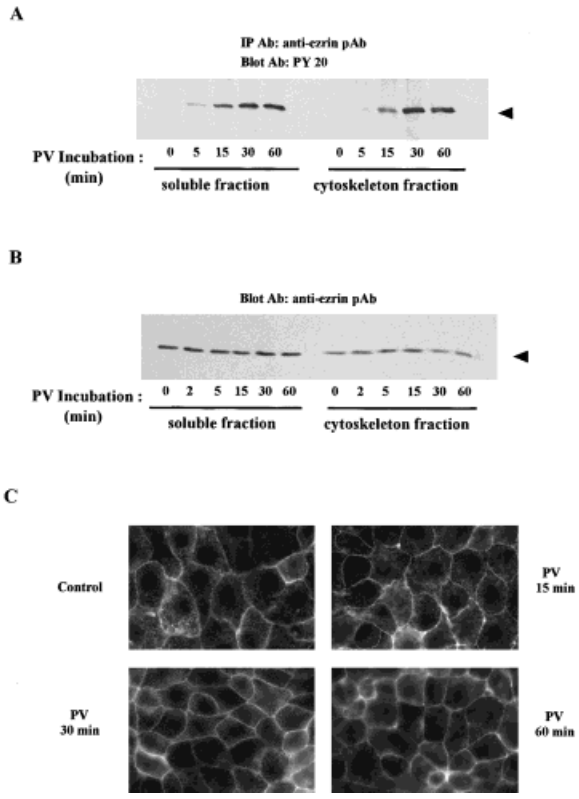

Fig. 5. Effect of PV stimulation on the association of ezrin with the cytoskeleton. **A:** MDCK cells were extracted with CSK-1 or CSK-2 buffers, and then divided into S- (soluble) and C- (cytoskeleton) fractions. Total ezrin in both S- and C-fractions was immunoprecipitated with antiezrin pAb. Immunoprecipitates were blotted with PY 20. **B:** Both S- and C- fractions were separated and blotted with antiezrin antibody. Arrow indicates the migration of ezrin. **C:** MDCK cells grown on glass coverslips were incubated with 100 mM PV for the indicated times. Cells were fixed and processed for immunofluorescence using rhodamine-phalloidin (actin) and then observed through an immunofluorescence microscope. Photographs were taken at a magnification of 1,000 ×.

fractions. A similar effect was observed in the total cell lysate (Fig. 2A). We next examined the distribution of ezrin in the S- and C-fractions after PV stimulation. The amount of ezrin recovered in the S- and C-fractions was estimated by comparing the staining intensity of each band on immunoblots. As shown in Fig. 5B, the amounts of ezrin recovered in the S- and C-fractions were unchanged after exposure to PV. These data indicate that the association of ezrin with the actin-cytoskeleton did not change after PV stimulation.

Furthermore, we examined the effect of PV treatment on the actin structure by Rhodamine phalloidin. The staining in the actin association with cell-cell junctions appeared unchanged (Fig. 5C). However, after incubation for 30 min, a decline in the staining of actin at the apical surface structure was observed (Fig. 5C). The similar effect was also observed in ezrin staining at the apical structure (Fig. 4D and P).

PV Treatment Induced Translocation of Cytosolic Ezrin to the Membrane Domain

The above findings indicate that when ezrin is activated by tyrosine phosphorylation in response to PV stimulation, cellular redistribution occurs, but the association with the actin-cytoskeleton is not changed. Because previous studies indicated that ezrin was localized to the cytoplasm, we examined whether PV treatment regulated the ezrin-plasma membrane interaction. For this purpose, we established a cell extract system, which was divided into cytosol and membrane fractions that permitted estimation of the amount of recovered ezrin. During a time-course of PV treatment, MDCK cells were homogenized and divided into cytosol and membrane fractions. Immunoblotting (Fig. 6A) revealed that the amount of ezrin recovered in the membrane fraction was increased after PV treatment, and the amount of ezrin recovered in the cytosol fraction was slightly decreased. Furthermore, lysis of PV-treated MDCK cells with RIPA buffer, and immunoprecipitation with antiezrin pAb showed that the amount of ezrin recovered in the membrane fraction was increased compared with that of untreated cells (Fig. 6B), and the amount of ezrin in the cytosol fraction of PV-treated MDCK cells was decreased compared with untreated cells. These data suggest that, when MDCK cells were treated

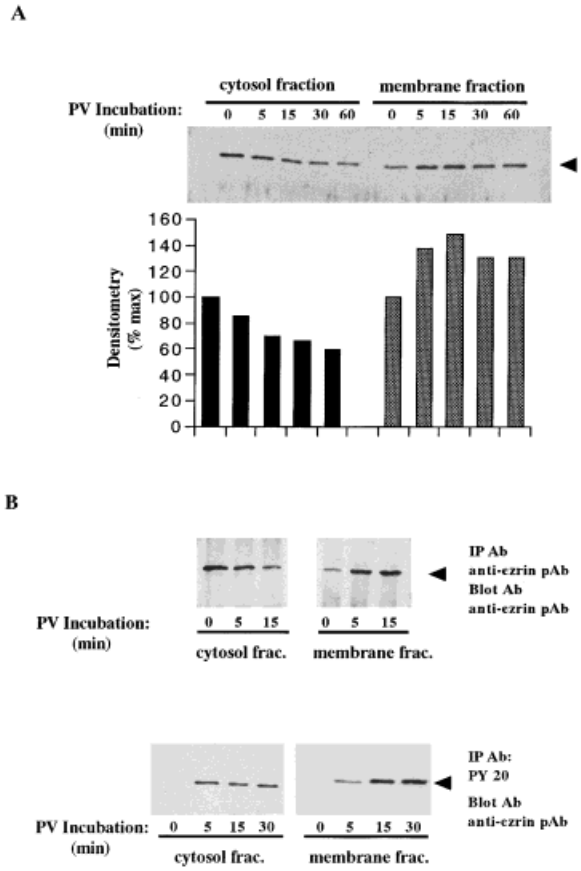

Fig. 6. Cytosolic ezrin is moved into the membrane domain after PV stimulation. **A**: MDCK cells were treated with 100 mM PV, homogenized, and divided into soluble (cytosol) and insoluble (membrane) fractions. Each fraction was resolved by SDS-PAGE, and ezrin was detected by immunoblotting with anti-ezrin pAb (upper panel). The lower panel shows the densitometric analysis of the immunoblotting. **B:** The soluble (cytosol) and insoluble (membrane) fractions of PV-treated or untreated MDCK cells were immunoprecipitated with antiezrin pAb (upper panel), or with PY 20 (lower panel). Each immunoprecipitate was immunoblotted with antiezrin pAb Arrows indicate the migration of ezrin.

with PV, cytosolic ezrin was translocated to the membrane fraction. In addition, the total tyrosine phosphorylate proteins were immunoprecipitated by PY 20 and the tyrosine phosphorylated ezrin was detected by immunoblotting. The results showed that the amounts of tyrosine phosphorylated ezrin recovered in both the cytosol and the membrane fractions were increased (Fig. 6B). However, the clearer increase was observed in the membrane fraction, suggesting that PV treatment induced a redistribution of tyrosine phosphorylated ezrin to membrane domain.

DISCUSSION

In this report, we examined how phosphorylation of ezrin was affected by treatment with tyrosine phosphatase inhibitors and if its cellular localization was altered. Our results demonstrated that treatment of MDCK cells with PV induced a marked increase in phosphorylation of ezrin at tyrosine residues, and a redistribution of ezrin to the membrane compartment. Interestingly, we obtained clear evidence that, following PV stimulation, ezrin was redistributed to the apical and lateral membranes. Furthermore, immunoblotting of cytosol and membrane fractions with antiezrin showed that, when MDCK cells were treated with PV, cytosolic ezrin was translocated to the membrane fraction. Because PV treatment can affect the cytoskeletal organization [Volberg et al., 1992], the association of ezrin with the cytoskeleton was also examined. The results showed that the distributions of ezrin did not change in the soluble and salt-sensitive cytoskeleton fractions after the PV treatment. Collectively, these findings demonstrate that in this model, PV treatment induced the increase in ezrin tyrosine phosphorylation and that only cytosolic ezrin was involved in the cellular redistribution and translocation to the membrane domain.

The phosphorylation of ezrin occurs in many systems and can induce various cellular responses. A correlation between the tyrosine phosphorylation-induced ezrin redistribution and changes in cell morphology has been demonstrated [Bretscher, 1989; Jiang et al., 1995]. Treatment of A431 cells with EGF induces a progression of morphological changes, including the rapid and transient formation of microvilli and membrane ruffles. Ezrin is recruited into the microvillar-like structures and membrane ruffles, and is phosphorylated on tyrosine and serine in a time course that parallels the formation and disappearance of these surface structures [Bretscher, 1989]. In the EGF treatment system, two tyrosine residues (Y 145 and Y 353) were phosphorylated [Krieg and Hunter, 1992]. HGF, also known as scatter factor, also induced morphological changes and tyrosine phosphorylation of ezrin, and shifted ezrin from the cytosol and generalized membrane to the areas of the ruffled membrane [Jing et al., 1995]. In this report, PV treatment induced a series of morphological changes and an increase in ezrin tyrosine phosphorylation, and ezrin was redistributed to the membrane structures. However, the results have some different patterns from those which were observed in EGF or HGF systems. As the PV treatment is not receptor-mediated, it only induced the cytoplasmic activation [Egerton et al., 1992; Huyer et al., 1997; Ruff et al., 1997]. In addition, ezrin is also an integral component involved in some cytoplasmic signaling pathways, such as the Rho pathway [Hirao et al., 1996; Takahashi et al., 1997] and the PI 3-kinase/AKT pathway [Gautreau et al., 1999]. It is possible that the activated form of ezrin in the PV treatment system might be different from that in the EGF and HGF treatment systems. PV stimulation of tyrosine phosphorylation of ezrin might be regulated by a cytoplasmic signaling pathway. In the present study, the major PV-induced tyrosine phosphorylation sites were not identified, and this remains to be established in the future. The reactivity of the antiphosphotyrosine antibody (PY 20) was apparently specific [Glenney et al., 1988). It did not seem important to question the assumption that PV treatment induced tyrosine phosphorylation of ezrin.

In epithelial cells, the adhesive interactions of cells with their neighbors are responsible for a wide variety of morphogenic and biochemical processes, and the subapical junctional complex and its regulation are involved in these processes [Gumbiner, 1996]. The tight junction (TJ), which seals together the plasma membranes of adjacent cells, acts as a barrier that separates apical and basolateral domains, and is responsible for the permeability barrier function in each epithelial cell. Below the TJ is the adherens junction (AJ), which connects sites for bundles of actin filaments and is formed by transmembrane adhesion proteins, cadherin family members, and cadherin-associated cytoplasmic proteins such as catenins, vinculin, α-actinin, and talin. Another class of cytoskeleton-associated epithelial junctions is the desmosomes, which is associated with intermediate filaments. The main targets for phosphorylation of tyrosyl residues in junctional components after PV treatment proteins, such as β-catenin, E-cadherin, ZO-1, and ZO-2, have been identified [Staddon et al., 1995; Volberg et al., 1992]. Thus, we suggest that PV treatment might have an effect on the tight junction or adherens junction compo-

nents. In addition, in ts-v-src-MDCK cells, ERM proteins were heavily phosphorylated in tyrosines in a time course similar to that of β-catenin, suggesting that the tyrosine phosphorylation of ERM proteins is involved in the regulation of cadherin-based cell adhesion [Takeda et al., 1995]. Our study showed that activation of ezrin by PV stimulation resulted in its redistribution to lateral cell-cell contact sites. However, it was not clear which intercellular junctional complex structure was involved. Because ezrin is an actin-associated protein, it is possible that it is moved to the nearby tight junction or adherens junction compartment in the cytoplasm after PV treatment. It was also reported that treatment of cells with PV (30 min at the 1 mM concentration) increased tyrosine phosphorylation of proteins at cellular junctions and induced deterioration of the adherens junction [Volberg et al., 1992]. The PV-induced downregulation of cellular contacts is thought to occur because tyrosine phosphorylation of these cytoskeleton-associated proteins disrupts the cytoskeleton and membrane adhesion molecules. However, in the present study, we obtained results that differed from those of previous reports: the downregulation of cellular contacts did not occur (Figs. 2B, 3B, and 4), and the association of ezrin with the cytoskeleton did not change during 60 min of PV treatment (Fig. 5B). Although downregulation of cellular contacts occurred after prolonged incubation (after two h, data not shown), the differences between the studies might have resulted from the different concentrations of PV used in this study.

Since PV has been reported to be involved both in the inhibition of PTPase activity and the activation of protein tyrosine kinase (PTK) cascade, we suggest that the enhancement of ezrin in tyrosine phosphorylation by PV may be mediated through the actions of PTK and PTPase. This may prove useful in the search for ezrin proteins controlled by tyrosine phosphorylation mechanisms, and in regulating cell adhesion and cortical mophogenesis.

ACKNOWLEDGMENTS

We thank Miss Maho Kohdabashi for her technical assistance.

REFERENCES

Algrain M, Turunen O, Vaheri A, Louvard D, Arpin M. 1993. Ezrin contains cytoskeleton and membrane binding domains accounting for its proposed role as a membrane-cytoskeleton linker. J Cell Biol 120:129–139.

Ayalon O, Geiger B. 1997. Cyclic changes in the organization of cell adhesions and the associated cytoskeleton, induced by stimulation of tyrosine phosphorylation in bovine aortic endothelial cells. J Cell Sci 110:547–556.

Berryman M, Gary R, Bretscher A. 1995. Ezrin oligomers are major cytoskeletal components of placental microvilli: a proposal for their involvement in cortical morphogenesis. J Cell Biol 131:1231–1242.

Bretscher A. 1989. Rapid phosphorylation and reorganization of ezrin and spectrin accompany morphological changes induced in A-431 cells by epidermal growth factor. J. Cell Biol 108:921–930.

Bush KT, Stuart RO, Li S-H, Moura LA, Sharp AH, Ross CA, Nigam SK. 1994. Epithelial inositol 1,4,5-trisphosphate receptors. J. Biol Chem 269:23694–23699.

Crepaldi T, Gautreau A, Comoglio PM, Louvard D, Arpin M. 1997. Ezrin is an effector of hepatocyte growth factor-mediated migration and morphogenesis in epithelial cells. J Cell Biol 138:423–434.

Egerton M, Burgess WH, Chen D, Druker BJ, Bretscher A, Samelson LE. 1992. Identification of ezrin as an 81-kDa tyrosine-phosphorylated protein in T cells. J Immunol 149:1847–1852.

Funayama N, Nagafuchi A, Sato N, Tsukita Sa, Tsukita Sh. 1991. Radixin is a novel member of the band 4.1 family. J Cell Biol 115:1039–1048.

Gautreau A, Poullet P, Louvard D, Aprin M. 1999. Ezrin, a plasma membrane-microfilament linker, signals cell survival through the phosphatidylinositol 3-kinase/Akt pathway. Proc Natl Acad Sci USA 96:7300–7305.

Gilbert-McClain LI, Verin AD, Shi S, Irwin RP, Garcia JG. 1998. Regulation of endothelial cell myosin light chain phosphorylation and permeability by vanadate. J Cell Biochem 70: 141–155.

Glenney JR, Zokas L, Kamps MP. 1988. Monoclonal antibodies to phosphotyrosine. J Immunol Methods 109:277–285.

Gumbiner BM. 1996. Cell adhesion: the molecular basis of tissue architecture and morphogenesis. Cell 84:345–357.

Helander TS, Carpen O, Turunen O, Kovanen PE, Vaheri A, Timonen T. 1996. ICAM-2 redistributed by ezrin as a target for killer cells. Nature Land 382:265–268.

Hirao M, Sato N, Kondo T, Yonemura S, Monden M, Sasaki T, Takai Y, Tsukita Sh, Tsukita Sa.1996. Regulation mechanism of ERM protein/plasma membrane association: possible involvement of phosphatidylinositol turnover and Rho-dependent signaling pathway. J Cell Biol 135:37–51.

Huyer G, Liu S, Kelly J, Moffat J, Payette P, Kennedy B, Tsaprailis G, Gresser MJ, Ramachandran C. 1997. Mechanism of inhibition of protein-tyrosine phosphatases by vanadate and pervanadate. J Biol Chem 272: 843–851.

Jiang WG, Hiscox S, Singhrao SK, Puntis MC, Nakamura T, Mansel RE, Hallett MB. 1995. Induction of tyrosine phosphorylation and translocation of ezrin by hepatocyte growth factor/scatter factor. Biochem Biophys Res Commun 217:1062–1069.

Krieg J, Hunter T. 1992. Identification of the two major epidermal growth factor-induced tyrosine phosphorylation sites in the microvillar core protein ezrin. J Biol Chem 267:19258–19265.

Laemmli UK. 1970. Cleavage of structural proteins during the assembly of the head of bacteriophage T4. Nature Land 227:680–685.

Luna EJ, Hitt AL. 1992. Cytoskeleton-plasma membrane interactions. Nature Land 258:955–964.

Mangeat P, Roy C, Martin M. 1999. ERM proteins in cell adhesion and membrane dynamics. Trends Cell Biol 9:187–192.

Ruff SJ, Chen K, Cohen S. 1997. Peroxovanadate induces tyrosine phosphorylation of multiple signaling proteins in mouse liver and kidney. J Biol Chem 272:1263–1267.

Staddon JM, Herrenknecht K, Smales C, Rubin LL. 1995. Evidence that tyrosine phosphorylation may increase tight junction permeability. J Cell Sci 108:609–619.

Stuart RO, Sun A, Bush KT, Nigam SK. 1996. Dependence of epithelial intercellular junction biogenesis on thapsigargin-sensitive intracellular calcium stores. J Biol Chem 271:13636–13641.

Takahashi K, Sasaki T, Mammoto A, Takaishi K, Kameyama T, Tsukita Sa, Tsukita Sh, Takai Y. 1997. Direct interaction of the Rho GDP dissociation inhibitor with ezrin/radixin/moesin initiates the activation of the Rho small G protein. J Biol Chem 272:23371–23375.

Takeda H, Nagafuchi A, Yonemura S, Tsukita Sa, Behrens J, Birchmeier W, Tsukita Sh. 1995. V-src kinase shifts the cadherin-based cell adhesion from the strong to the weak state and β-catenin is not required for the shift. J Cell Biol 131:1839–1847.

Takeuchi K, Sato N, Kasahara H, Funayama N, Nagafuchi A, Yonemure S, Tsukita Sa, Tsukita Sh. 1994. Perturbation of cell adhesion and microvilli formation by antisense oligonucleotides to ERM family members. J Cell Biol 125:1371–1384.

Tsukita Sa, Oishi K, Sato N, Sagara J, Kawai A, Tsukita Sh. 1994. ERM family members as molecular linkers between the cell surface glycoprotein CD44 and actin-based cytoskeletons. J Cell Biol 126:391–401.

Volberg T, Zick Y, Dror R, Sabanay I, Gilon C, Levitzki A, Geiger B. 1992. The effect of tyrosine-specific protein phosphorylation on the assembly of adherens-type junctions. EMBO J 11:1733–1742.

Warne TR, Buchanan FG, Robinson M. 1995. Growth-dependent accumulation of monoalkylglycerol in Madin-Darby canine kidney cells. Evidence for a role in the regulation of protein kinase C. J Biol Chem 270:11147–11154.

Wilden PA, Broadway D. 1995. Combination of insulinomimetic agents H_2O_2 and vanadate enhances insulin receptor mediated tyrosine phosphorylation of IRS-1 leading to IRS-1 association with the phosphatidylinositol 3-kinase. J Cell Biochem 58:279–291.

Wu Y-X, Uezato T, Fujita M, Fujita K. 1996. Immunocytochemical study of ezrin in cultured Madin-Darby canine kidney cells. Biomedical Res 17:465–471.

Yonemura S, Hirao M, Doi Y, Takahashi N, Kondo T, Tsukita Sa, Tsukita Sh. 1998. Ezrin/radixin/moesin (ERM) proteins bind to a positively charged amino acid cluster in the uxta-membrane cytoplasmic domain of CD44, CD43, and ICAM-2. J Cell Biol 140:885–895.